PRECIPITATE COARSENING AND GRAIN GROWTH IN STEELS

K. C. Russell
Department of materials science and Engineering
Department of Nuclear Engineering
Massachusetts Institute of Technology
77 Massachusetts Avenue
Cambridge, MA 02139-4307

Abstract

Precipitate coarsening and grain growth are ubiquitous in austenite and its decomposition products. Grain growth in austenite and ferrite is limited by particle pinning and by solute segregation at grain boundaries. Progress has been made in the modeling of grain growth and some experimental verification has been made.

Particulate phases are important in ferrite and austenite, both for strengthening and for grain size control. The theories for particle coarsening are in general agreement with one another and with experimental data.

Introduction

Steel has played a key role in human societies since its discovery some 3500 years ago. Certainly the early blacksmiths observed the effects--mostly deleterious--of overheating of steel during forging. The most notable effects were probably (in today's terminology) the loss of hardness with the coarsening of carbides produced during tempering and the deleterious effects of overheating austenite on the properties of subsequent phases.

Coarsening and grain growth both refer to the parasitic surface energy driven evolution of a system of particles to larger mean sizes. Coarsening refers to the evolution of a system of precipitate particles embedded in a matrix. In grain growth the particles abut one another and are not separated by a matrix phase.

This paper deals with grain growth in austenite and ferrite and the coarsening of compound precipitates. The latter include both temper carbides and other compounds used in strengthening and in control of grain size in austenite and ferrite.

The complexities of coarsening and grain growth theory are more appropriate in a paper written for theoretical physicists than in this contribution, which is directed toward physical metallurgists. The theories described are at the simplest levels, which incorporate the basic physics of coarsening. Those interested in the complexities may find help in this paper's references or search the literature under the names of the leaders in coarsening theory. Among these are J. W. Cahn, M. Hillert, Lücke, and V. V. Slyozov (also spelled Slezov).

Theory

Precipitates:

The theory of diffusion in solids dates back at least to Fick (1) in 1855. Analytical solution of the second order partial differential equation which is Fick's second law is generally impossible,

especially in three dimensions. However Zener (2) presented an elegant analysis of the growth rates of plates, cylinders, and spheres from supersaturated solid solutions. He found in each case that the size of the particle varied as $(Dt)^{1/2}$ times an appropriate function of the solute concentrations in the particle and matrix. Here, D = diffusion coefficient and t = time. Zener's formulations are the basis for much subsequent work in precipitate growth and coarsening.

The basic coarsening theories (3-5) assume a small volume fraction of spherical, strain-free solid solution precipitates which grow or shrink at a rate controlled by diffusion through the matrix. Rapid diffusion paths such as dislocations and grain boundaries are assumed not to play a role. Later derivations have attempted to relax these approximations.

The basic physics behind particle coarsening are illustrated in a simple, unpublished derivation by R. L. Coble (6) who focused on the behavior of the largest particles, those with $r = r_{max}$. He assumed that:

a. The maximum particle size, r_{max} and the mean, $\bar{r}$, are related by a constant factor, β, so that:

$$r_{max} = \beta\ \bar{r} \qquad (1)$$

b. The concentration gradient at the particle:matrix interface for a particle of size r_{max} is given by:

$$\Delta C/\Delta r = [C(\bar{r}) - C(r_{max})]/r_{max}. \qquad (2)$$

This result comes from diffusion theory and is clear in Zener (2).

c. The solute concentration at the particle:matrix interface is increased above the equilibrium value, C_e according to the Gibbs-Helmholtz equation:

$$C(r_{max}) = C_e \exp.(2\gamma V_m/ r_{max}\ RT) \qquad (3)$$

where γ = particle:matrix interfacial energy, V_m = molar volume in the particle, and

RT = gas constant times temperature.

Expansion of the exponential gives

$$C(r_{max}) = C_e(1 + 2\gamma V_m/ r_{max}\ RT) \qquad (4)$$

A similar equation applies for $C(\bar{r})$.

d. The mass flux at the particle:matrix interface, J, is given by

$$J = -D \frac{\partial C}{\partial r})_{r_{max}} \qquad (5)$$

e. The flux and particle growth rate are related by:

$$\dot{r}_{max} = JV_m \qquad (6)$$

It is a simple to combine equations 1-6 and integrate to give:

$$\bar{r}^3 - \bar{r}_0^3 = \frac{6DC_e\gamma V_m^2 t}{\beta^3 RT} \qquad (7)$$

where $\bar{r}_0$ = starting particle size and t = time. From experiment β is the order of 2.

The theory of diffusion controlled precipitate coarsening was developed by Greenwood (3), Wagner (4), and Lifshitz and Slyozov (5). The derivations are too lengthy to repeat here, but the resulting rate equation is:

$$\bar{r}^3 - \bar{r}_0^3 = \frac{8DC_e\gamma V_m^2 t}{9RT} \qquad (8)$$

Theory also predicts that the particles will take on a time-independent size distribution, as shown in Figure 1, with a limiting particle size of:

$$r_{max} = 1.5\,\bar{r} \qquad (9)$$

Equations 7 and 8 are in agreement if $\beta = 3^{4/3}/2$. The simple Coble treatment is thus in close agreement with the rigorous analysis.

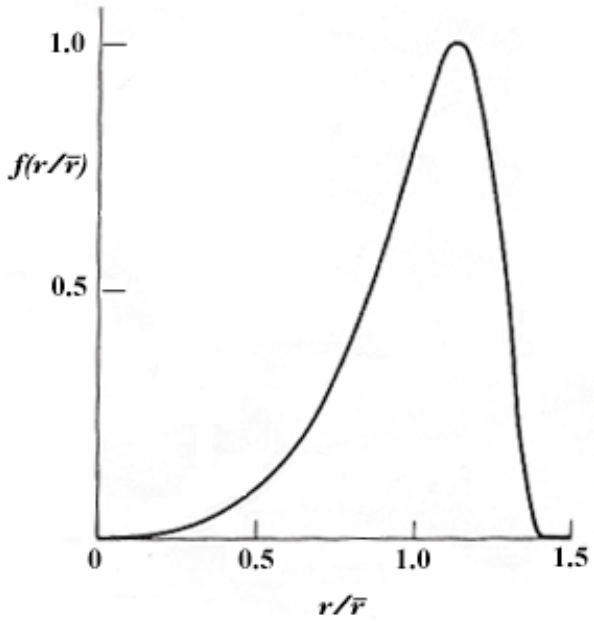

Figure 1. Final steady state normalized particle size distribution for diffusion-controlled coarsening. (After Martin, et al. 7)

The most striking aspect of equation 8 is that the mean radius cubed varies as time, as opposed to the radius squared in growth calculations. Coarsening is thus a much slower process than precipitate growth, as is reasonable in that growth of one particle only occurs by cannibalizing other particles. It is also seen that the key material variables are solubility and diffusion coefficient. A system of sparingly soluble particles made of a slow diffusing solute will be stable against coarsening. The interfacial energy is likely to be near 0.1 J/m^2, and the molar volume about 10^{-5} m^3/mole: variations in V_m and γ are thus not likely to have a key role in coarsening behavior.

Second phase particles of interest in steels are largely carbides, nitrides, carbonitrides, oxides, and sulfides rather than solid solutions. At least two diffusivities and two concentrations are involved in determining the coarsening behavior. Their coarsening behavior clearly cannot be described by equation 8: an extended treatment is needed.

The coarsening rate of compound precipitates was analyzed by Björklund, et al (8) and by Bhattacharyya and Russell (9). The former paper was concerned with mixed alloy carbides in steel, whereas the latter was concerned with stoichiometric particles in any alloy. Although the approaches are different, the results are very similar for the coarsening of alloy carbide particles in steel.

The Bhattacharyya and Russell derivation is easily outlined for the case of AB precipitates in a matrix, N. (Non-unity stoichiometric coefficients complicate the analysis without much altering the end coarsening equation.)

The condition for equilibrium at the particle: matrix interface is now

$$C_A^r C_B^r = K_e \exp.(2\gamma V_m/rRT) \qquad (10)$$

Where $K_e = C_A^\infty C_B^\infty$ is the equilibrium constant for A and B solubility over bulk AB in the matrix. C_A^∞ and C_B^∞ are the concentrations far from the precipitate particle.

Maintenance of the 1:1 stoichiometric ratio requires that the fluxes of A and B atoms to or from the particles be equal. This equal flux condition will almost always be easier satisfied for one species than the other. If $C_A^\infty > C_B^\infty$ and $D_A > D_B$, the concentration of A will be constant right up to the surface of the particle, whereas there will be a concentration gradient in B. B is then the rate controlling species.

In either event the coarsening equation may be expressed as:

$$\bar{r}^3 - \bar{r}_0^3 = \frac{8 < DC > \gamma V_m^2 t}{9RT} \qquad (11)$$

Björklund, et al. were concerned with the coarsening of alloy carbides so that <DC> equals $D_A C_A$ times compositional factors usually not far different from unity. Here A refers to the alloy element, which would be a carbide former such as Cr, W, or Mo, and B to carbon. In the Bhattacharyya and Russell treatment,

$$<DC> = D_A C_A^\infty \text{ or } <DC> = D_B C_B^\infty \qquad (12)$$

which ever is the smaller. The two treatments are thus largely equivalent for the coarsening of alloy carbides in steel. The Björklund, et al treatment has the advantage of not assuming stoichiometric carbides.

Earlier Cochart (10) presented an approximate analysis of compound particle coarsening, which gave the correct time dependence of coarsening and reflected the importance of the solubility. Wagner (4) suggested the criterion for identifying the rate controlling species. This early work was not widely appreciated.

In the general case, and especially when both A and B diffuse substitutionally, the rate controlling species could be either element. In the case of alloy carbides, a substitutional alloy element will diffuse much slower than will the interstitial carbon. It is thus unlikely that any disparities in matrix concentration will cause the carbon to be rate controlling.

Lee, et al. (11) presented an analysis of precipitate coarsening of multicomponent particles, which generalized and extended the treatment of Björklund, et al. Their analysis showed that coarsening could be viewed in terms of a series resistance composed of the resistances to coarsening provided by the various components in the particle. They found that each component, no matter how plentiful or how fast diffusing, increased the coarsening resistance. If, however, the product DC were much less for one component than any of the others, it would become rate controlling. The criterion of Bhattacharyya and Russell would then apply. Their criterion (equation 12) may be looked upon as selecting the largest resistance in the series circuit and equating the rest to zero.

The various parameters and constants in equation 11 may be combined to give:

$$\bar{r}^3 - \bar{r}_0^3 = K_c t \qquad (13)$$

Where K_c= rate constant for coarsening, which depends strongly on temperature through the diffusivities and possibly the particle solubility.

Grain Growth:

Grain growth occurs in polycrystalline arrays so as to reduce the total grain boundary energy. (The energy of external surfaces may be an important factor in grain growth in thin sheets.) Many experimental and theoretical studies of grain growth have been performed over the years. Reviews include those by Burke and Turnbull (12) and Thompson (13).

The following simple analysis considers a pure, one component materials with grain boundaries of isotropic mobility. The particle is surrounded by grains averaging the overall mean size. A grain smaller than the mean will shrink, a larger one will grow.

A polyhedral grain is approximated by a sphere of equal volume, for which the area varies as dA/dV = 4/D, where D = diameter of the equivalent sphere. If the grain changes volume by dV, the change in grain boundary energy is (4γ /D) dD, where γ = grain boundary energy per unit area. The decrease in grain boundary energy of the adjacent grains must be proportional to $1/\overline{D}$, so that the change in the grain boundary energy is ($4\alpha\gamma / \overline{D}$) dD , where α = a numerical constant. If D = $\overline{D}$, the change in surface energy must be zero. Hence, $\alpha = 4$ and the change in free energy due to growth of the subject grain is:

$$\frac{dG_1}{dV} = 4\gamma\frac{1}{D} - \frac{1}{\overline{D}} = P_1 \qquad (14)$$

where P_1 is the corresponding driving pressure. The growth rate of a grain is given by $\dot{D}$ = MP_1/RT where M = grain boundary mobility. It is convenient to follow the growth of the largest particle, that having $D = D_{max}$. We assume that $D_{max} = \beta\overline{D}$, that maximum and mean grain diameters have a constant ratio throughout grain growth. Using this ratio and standard derivations of M gives:

$$\overline{D}^2 - \overline{D}_o^2 = [\frac{8\gamma V_M D_b}{RTa}\left(\frac{1-\beta}{\beta^2}\right)]t \qquad (15)$$

Where a = lattice parameter and D_b = diffusivity of atoms across the grain boundary. Burke and Turnbull (12) derived a similar equation, though with an undetermined numerical constant. This $\overline{D}^2$ vs. t relationship is obtained in other, more rigorous treatments of grain growth.

Hillert (14) used an elegant analysis to show that $D_{max} = 2\overline{D}$. Then:

$$\overline{D}^2 - \overline{D}_o^2 = \frac{2\gamma V_M D_b}{RTa} t \qquad (16)$$

Equation 16 does not reflect the retarding effect of solutes and precipitate particles on grain growth. It is thus something of an upper limit for $\overline{D}$. Grain sizes predicted by equation 16 are often far greater than those observed in engineering alloys and even commercially pure materials.

Fine second phase particles have long been known to limit grain growth by pinning the grain boundaries. The theory for this phenomenon goes back at least to C. S. Smith (15) in 1948, who was acting on a suggestion by C. Zener. Many analyses of the phenomenon have been published in the intervening years. The following simple extension of the derivation for equation 16 illustrates some of the physics.

Let an alloy have a volume fraction f_v of uniformly distributed second phase particles of diameter, D_p. By the principles of quantitative metallography these particles will occupy an area fraction of f_v on the grain boundaries of the system. Movement of the grain boundary requires pulling away from the pinning effects of these particles. The grain boundary no longer exists on the area occupied by the particles, hence must be re-created as the boundary pulls away. The free energy change, or pressure on pulling the boundary away from these particles during growth is given by:

$$dG_2/dV = 3f_v\gamma/D_p = P_2 \qquad (17)$$

Grain growth will stop when the free energy to pull the boundary away from the particles equals the free energy gained through decrease in grain boundary energy, or $P_1 + P_2 = 0$. Grain growth will cease at critical value of D, given by:

$$\frac{D_{max}}{D_p} = 4(\frac{D_{max}}{\overline{D}} - 1)/3f_v \qquad (18)$$

The ratio $\frac{D_{max}}{\overline{D}}$ must obviously be greater than unity, and must be less than two to prevent runaway grain growth. Taking a value of 1.5 yields

$$\frac{D_{max}}{D_p} = \frac{2}{3} f_v^{-1} \qquad (19)$$

Equation 19 indicates that ca. one volume percent of nanometer sized particles will limit grain size to the hundreds of nm range.

Hillert (14) made an elegant analysis of grain growth which somewhat paralleled that for diffusional coarsening leading to equation 8 and Figure 1. He found that a particle for which $D>2\overline{D}$ would grow without limit. Such particles therefore could not exist in so-called normal grain growth, which requires a steady-state size distribution, when normalized to mean grain

size. Thus, $D_{max} = 2\overline{D}$. His statistical treatment also derived a particle size distribution in grain growth similar to that for diffusion-controlled particle coarsening.

Hillert also integrated the effects of second phase particles into his analysis of the evolution of the grain size distribution and found that a steady state particle size distribution was unattainable in the presence of particle pinning.

Abbruzzese and Lücke (16) developed a statistical theory of grain growth claimed to be more rigorous than earlier efforts. The particle pinning term was left as a parameter. Their predictions of the effects of pinning on grain growth differed significantly from those of Hillert (14). Later authors used the Abbruzzese and Lücke pinning term as a parameter in data fitting.

Numerical simulation is often used to describe the kinetics of grain growth. Most simulations have been used to describe two dimensional grain growth, as may occur in sheet and thin films. Numerical simulation is a much more difficult task in three dimensions. Most simulations of 3-D grain growth have been performed in the last ten years, as facilitated by ever greater algorithm sophistication and computing power. There have been several very different approaches to simulation of 3-D grain growth. (See Krill and Chen 17)

This paper will discuss only the so called phase-field simulation model that uses an order parameter to distinguish between grain orientations. It is obviously impossible to characterize each and every one of the myriad of possible misorientations between adjacent grains. Krill and Chen (17) assign from 10-100 different order parameters (Q) to distinguish between the various possible orientations. If adjacent grains have different Q's, they remain discrete. If the Q's are the same, the two grains coalesce to form a single, larger grain. A gradient energy model was used for grain boundary energy, and the rate constants in their growth equations were related to the grain boundary mobility.

An increase in the number of order parameters leads to a disproportionate increase in computational time. A computationally convenient number of parameters, say Q =10, leads to coalescence. The authors note that coalescence is not observed experimentally, hence should not appear in the simulation. Use of a much larger number of order parameters eliminates grain coalescence, but at an unacceptable increase in computer time.

Krill and Chen (17) escaped this dilemma by using a small number of order parameters, and reassigning all the parameters at any threat of coalescence. Figure 2 illustrates the effects of such reassignment. The differences in the progression of area per grain with time for Q = 20 and Q = 100 fixed parameters are due to coalescence. Using only 20 parameters and reassigning them to avoid coalescence is seen to give almost the same result as Q = 100, without reassignment, at a significant saving in computation. It is noted that either simulation produces the familiar $\overline{D}^2$ vs. t relationship. The two differ at early times due to nucleation at early times in the Q = 100 case.

The authors state that simulation efforts that include impurity effects and use a spectrum of boundary energies and mobilities are in progress, but are apparently far from fruition.

Solute Drag On Grain Boundaries: Ultra-pure zone refined metals undergo rapid recrystallization and grain growth at temperatures where the microstructure in the commercially pure metal changes little in years. There have been numerous attempts to analyze the effect of solutes on grain boundary mobility. Perhaps the most notable are those by Cahn (18) and by Lücke and Stüwe (19). That of Cahn will be very briefly described here.

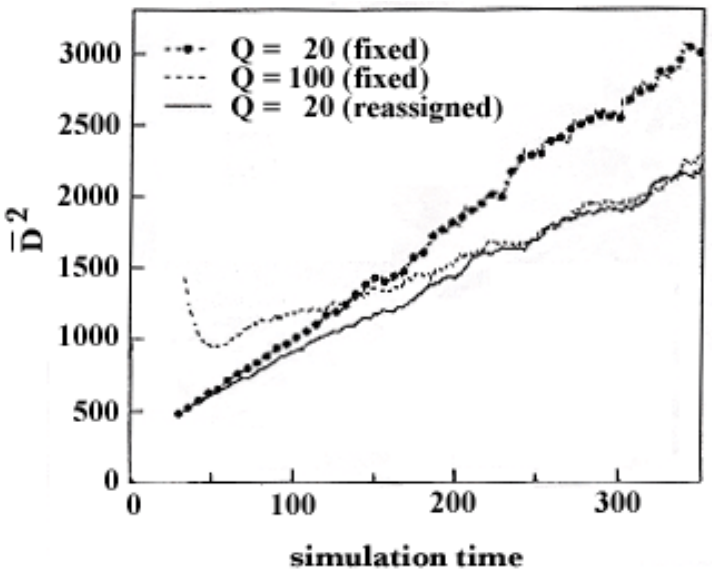

Figure 2. Time evolution of the square of average gain size with simulation time. Q = number of order parameters used to distinguish various grain orientations. (After Krill and Chen 17)

In the simplest case adsorption and rapid diffusion are restricted to a one-atom thick region in the boundary. Cahn relaxed this assumption so that solute was assumed to be attracted to the grain boundary by a triangular potential well. The equilibrium solute concentration was then related to the potential by a Boltzmann distribution.

A stationary grain boundary tends to equilibrate with the matrix and become enriched with solute. Any displacement of the grain boundary would tend to force solute atoms into higher energy sites, thus producing a free energy gradient. This gradient translates into a pressure, which would tend to move the grain boundary back to its original position. Migration of the grain boundary would thus only occur in the presence of another, greater pressure.

At very low migration velocities, the solute may diffuse along with the boundary and maintain nearly the equilibrium concentration. There is thus a very small solute drag force. Conversely, at high boundary velocities the solute atmosphere would be left behind, where it could not interact with the boundary. Cahn also found a breakaway phenomenon. At a sufficiently high velocity the boundary would break away from the atmosphere and suddenly increase its velocity. The boundary mobility would approach that for a clean boundary and grain growth kinetics could approach the idealized state described by equation 16. Fast diffusing solutes would the last to be left behind, hence would have the greatest retarding effect.

The theory makes notable predictions in the low velocity regime. First, the velocity varies inversely as the solute concentration, so that minor solutes have a very large effect. Secondly, slower diffusing elements are least able to keep up with the slow-moving boundary, hence have the greatest retarding effect.

Combination of the solute drag effects with either the analytical or computational grain growth analyses given early would give an extremely important result. Unfortunately, such a treatment seems very far from feasible at present.

EXPERIMENTAL

Particle coarsening measurements are time consuming and difficult. It is not always easy to separate nucleation from growth, to determine just what phase has nucleated or to determine the nucleation site. Most information is obtained from polished sections, which is a tedious, time consuming job.

Compound Precipitates:

The coarsening of compound precipitates plays an important role in the physical metallurgy of steel. Coarsening of temper carbides in martensitic steels, of sulfides and nitrides in the annealing of electrical steel, of nitrides in plain carbon steel, and of carbonitrides in High Strength Low Alloy (HSLA) steels are some examples.

Bhattacharyya and Russell (20) used Cu-SiO_2 as a model system. Internal oxidation of a Cu-0.11 wt.% Si alloy produced SiO_2 particles with a mean size of about 20 nm. Coarsening took place for times up to 5×10^5 s at temperatures from 850 ^oC to 1000 ^oC. Resulting particle size distributions were roughly similar to the theoretical shape shown in Figure 1, but in all cases had long tails at sizes larger than $2\bar{r}$. Coarsening in all cases followed a $\bar{r}^3$ vs. t law, and activation plots of the coarsening rate constant were linear.

The authors tried to set the oxygen content in the matrix (and thereby the silicon content) by the coarsening atmosphere. They concluded that they had failed, and that the solute concentrations remaining were set during internal oxidation. Accordingly, they were not able to determine theoretical values of K_c to compare with their measured values. Agreement on the other theoretical predictions was encouraging.

Ozaki and Zee (21) studied the coarsening of HfC particles in a W matrix. Their results are illustrative. They studied a system of about 0.4 mol % of intragranular HfC particles with a starting size of ca. 20 nm. Hf is a fast diffuser in W with an activation energy given as about 335 kJ/mole, as opposed to their stated 480 kJ/mole for self diffusion of W. Ozaki and Zee appeared puzzled that the activation energy of coarsening corresponded to that for self diffusion of W.

Hillert (22) analyzed intragranular precipitation of graphite in a steel. He showed that for small particle sizes Fe diffusion was the rate controlling process, and only at large sizes was C diffusion rate controlling.

The higher activation energy observed by Ozaki and Zee (21) is thus to be expected. It is not enough to diffuse Hf from small particles to large in order to effect coarsening. It is also necessary to diffuse W out of the way so that the Hf will have a place to re-precipitate. The 480 kJ/mole activation energy for coarsening is thus consistent with theory.

Gustafson (23) studied the coarsening behavior of TiC particles in austenitic stainless steel. The TiC particles contained small amounts of the other elements. Coarsening was at 900 ^oC for times up to 2.4×10^7 s. Particles had a mean radius of 51 nm at the start and 75 nm after the longest anneals so the amount of coarsening was thus not great. Calculated rates were from a computerized system based on the series resistance model discussed earlier and a multicomponent diffusion theory by Morral and Purdy (24). The theory predicted that the presence of nitrogen in the TiC precipitates would reduce the coarsening rate by an order of magnitude as compared to the coarsening of pure TiC. Agreement between model and experiment were found for an assumed surface tension of 0.2 J/m^2. Such an interfacial energy is physically reasonable so that the agreement is rewarding.

Temper carbides based on such refractory metals as W and Mo are observed to coarsen little, even at red heat where plain iron carbide would coarsen instantly. Such is the basis of so-called hot working tool steels. Either theory described earlier may be used to calculate such coarsening. It is easy to calculate that at 923K an iron carbide particle coarsening by carbon diffusion will go from the nm range to a tenth micron in seconds. The coarsening of an alloy carbide will be controlled by diffusion of the alloy element in the matrix. Such carbides are predicted to take days or years to go from nm to a tenth micron. This simple calculation illustrates the physical basis for hot-working, or red-hardness steels. This behavior is shown in Figure 3, from Bain (25)

The most thorough study of the coarsening of alloy carbides was by Lee, et al. (11, 26, 27). They studied a commercial alloy and four experimental alloys with Mo_2C-based precipitates. Each alloy contained about 0.2 wt.% C, significant amounts of Co, Ni, and Mo, and in three cases, Cr. The precipitates were rod shaped so the coarsening theory had to be modified. The cube of the rod length was found to be linear in time as is expected for volume diffusion controlled coarsening.

Comparison with theory was based on the series resistance model of Lee, et al described earlier. Mixed Mo-Cr carbides were expected in the Cr-bearing steels so the coarsening rate constant would depend on the diffusivities of both elements. Good agreement between theory and experiment was found for coarsening rate calculations based on the diffusion of Mo in ferrite for the Cr-free steel. In addition the activation energy for coarsening was close to that for Mo diffusion in ferrite. This extensive study lends considerable support to the theory for coarsening of compound precipitates.

Grain Growth:

High temperature grain growth in very pure elemental metals is sometimes reasonably well described by equation 16. The inability to predict grain growth rates under other conditions is due in large part to ignoring the retarding effects of solutes and second phase particles.

The simulation of Krill and Chen (17) described earlier cannot give absolute values of grain size, but the relative values predicted agree well with experiment and earlier analytical calculations. Figure 2 shows a $\overline{D}^2$ vs. t relationship. The analysis also predicts such topological parameters as faces, edges, and vertices per grain. The predictions are in reasonable agreement with measurements on several steels and non-ferrous alloys.

Austenite: Austenite grain size exerts a major influence on the microstructure and properties of subsequent transformation products. Grain size is also an important characteristic of steels used in the austenitic state, as is the case for many stainless steels.

Figure 4 compares predictions of grain size distributions by Krill and Chen (17) and by Hillert (14) with experimental results on type 304 austenitic stainless steel. Krill and Chen claim that their model is in better agreement with these data than that of Hillert. Neither distribution gives nearly an exact fit, which is entirely reasonable in view of the approximations in both treatments

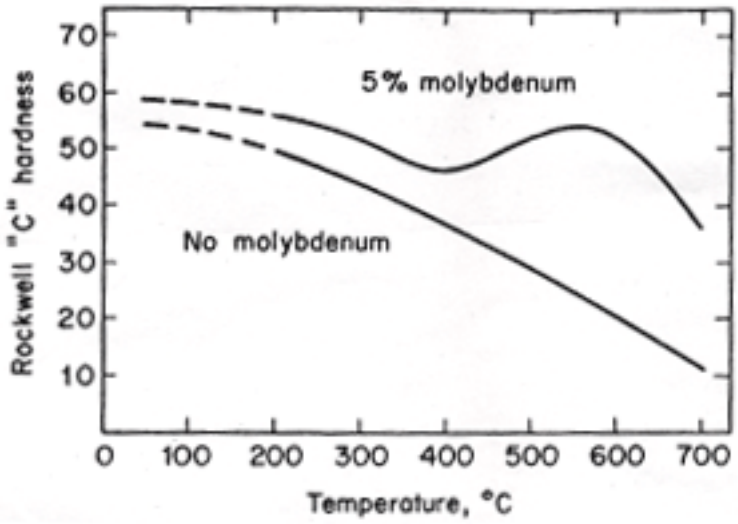

Figure 3. Secondary hardening in steel containing 0.34 wt.% C. (After Bain 25)

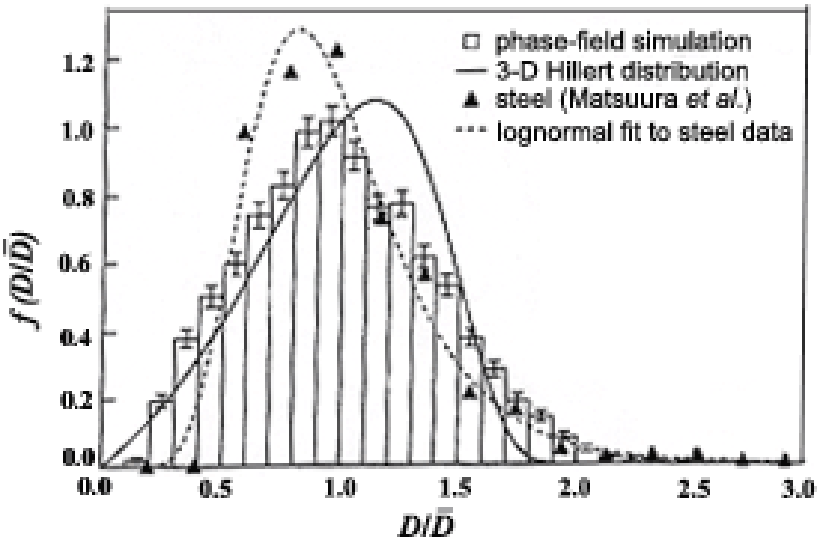

Figure 4. Comparison of grain size distributions measured on a type 304 austenitic stainless steel and those predicted by Hillert (14) and by Krill and Chen (17). (After Krill and Chen 17)

A recent paper by Militzer, et al. (28) illustrates some important characteristics of austenite grain growth. In particular they related theoretical predictions to experiments on commercial alloys.

The paper studied coarsening in three commercial Al-killed plain carbon steels. Carbon contents were 0.038 wt.%, 0.17 wt.%, and 0.78 wt.%. Austenite grain growth was studied in isothermal, stepped, and continuous cooling tests. The latter testing conditions were utilized to better model grain growth during rolling operations. Only the easier to interpret isothermal tests will be considered here.

Isothermal studies were made at temperatures from 850 ^{o}C to 1150 ^{o}C. Measurements on polished sections were converted to true 3-D grain sizes and in some cases to grain size distributions. Grain sizes ranged from typically tens of μm at the start of the annealing to hundreds of μm at the end.

The experimental results were analyzed in terms of a statistical grain growth theory by Abbruzzese and Lücke (16). The effects of particle pinning on grain growth are accounted for by a pinning parameter, P.

Militzer, et al. used P as a fitting parameter accounting for both particle pinning and solute drag to force agreement between theory and experiment. The parameter, P, was found to be linear in temperature and time-independent in the higher carbon steels, but showed a more complex behavior in the low carbon steel. In this latter case, P had a complicated dependence on temperature and varied with time. A time dependent P would be needed to describe AlN particle dissolution.

Figure 5 shows that the lower carbon steels have an asymptotic approach to a limiting grain size, as predicted by the Zener-Smith theory. Figure 6 shows the comparison of the theoretical and experimental maximum grain radii. The agreement is impressive.

The AlN particles responsible for boundary pinning were eliminated in the lowest carbon alloy by heating above 1150 ^{o}C, where dissolution occurred. Subsequent heating during grain growth experiments was thought to be too brief to allow re-precipitation. Unpinned austenite growth was then studied at 1050 ^{o}C. The effect of the unpinning was dramatic. First, grain growth followed a simple, parabolic law with no approach to a limiting grain size. Second, the grain growth was much faster than in the presence of pinning. Grains in the unpinned alloy quadrupled in size in 100 sec. going from 50μm to 200μm. Grains in the pinned alloy grew hardly at all under the same treatment. Even in the unpinned alloy grain growth was much slower than predicted by the simple theory, probably due to solute drag on the grain boundaries.

HSLA steels are low in carbon (0.05-0.15 wt.%) with small amounts of strong carbide-forming elements such a niobium, vanadium, or titanium. With proper processing these steels have twice the strength of mild steels. This doubling of strength at a relatively low cost has made these alloys very popular and a subject of intensive research (Hansen, et al. 30)

The alloying additions give copious fine (nm to a few tens of nm) carbonitride particles whose primary role is in limiting austenite grain growth during processing. The particle pinning gives finer grained austenite than would normally be obtained. Figure 7 shows the strong delaying effect of small Nb and V additions on austenite recrystallization.

Ferrite nucleates largely on austenite grain boundaries, hence also has finer grains and higher strength. HSLA steels may have ferrite grain sizes of ca. 5 μm as compared to 20-30 μm characteristic of plain carbon steel. The resulting Hall-Petch grain size strengthening is largely responsible for the doubling of the strength. The particles also provide some precipitation hardening of the steel.

Coarsening of the carbonitrides is clearly controlled by the mobilities of the carbide formers, which being substitutional, diffuse slowly. The success of HSLA steels shows that the coarsening of the carbonitrides during processing is not excessive. Quantitative tests of particle coarsening in HSLA steels are yet to be done.

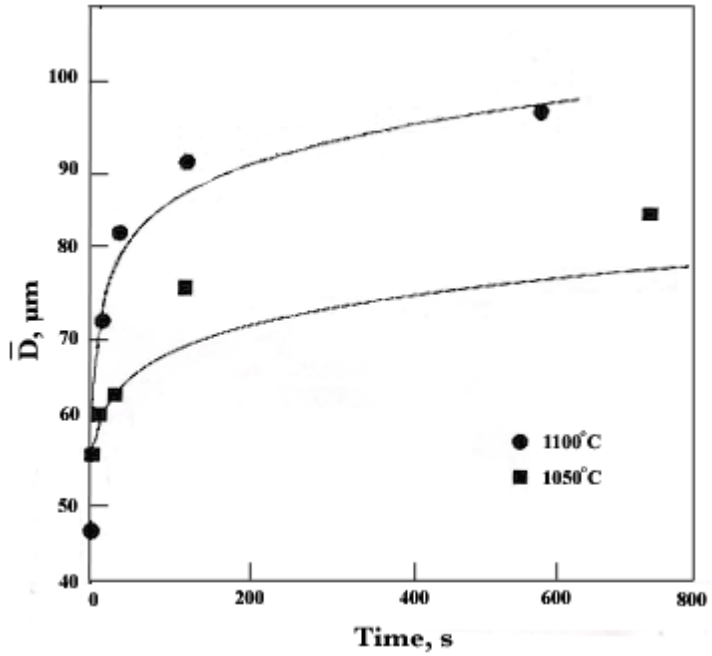

Figure 5. Austenite isothermal grain size kinetics in an Al-killed 0.17 wt.% C plain carbon steel. Continuous lines are from the theory of Abbruzzese. and Lücke. The degree of particle pinning of the grain boundaries was used as a fitting parameter. (After Militzer, et al. 29)

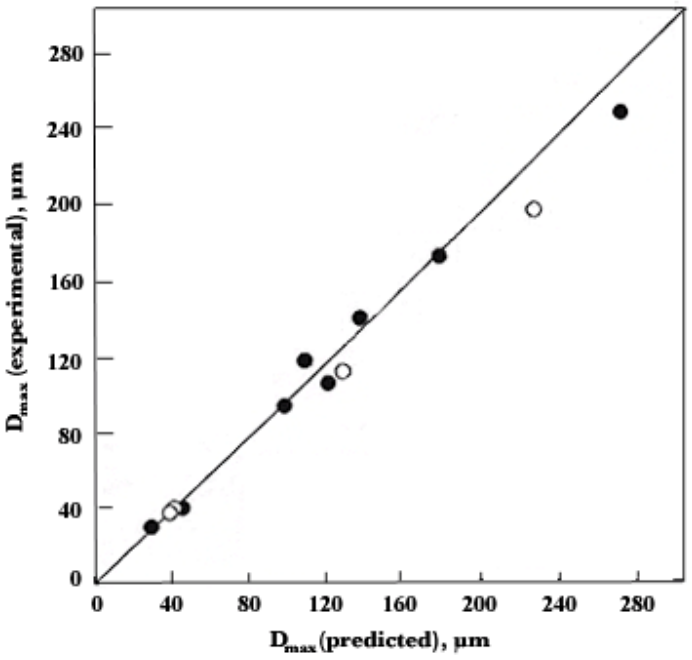

Figure 6. Comparison of limiting grain sizes in two plain carbon steels with those predicted by the Zener-Smith criterion. Close agreement is seen. (After Militzer, et al. 29)

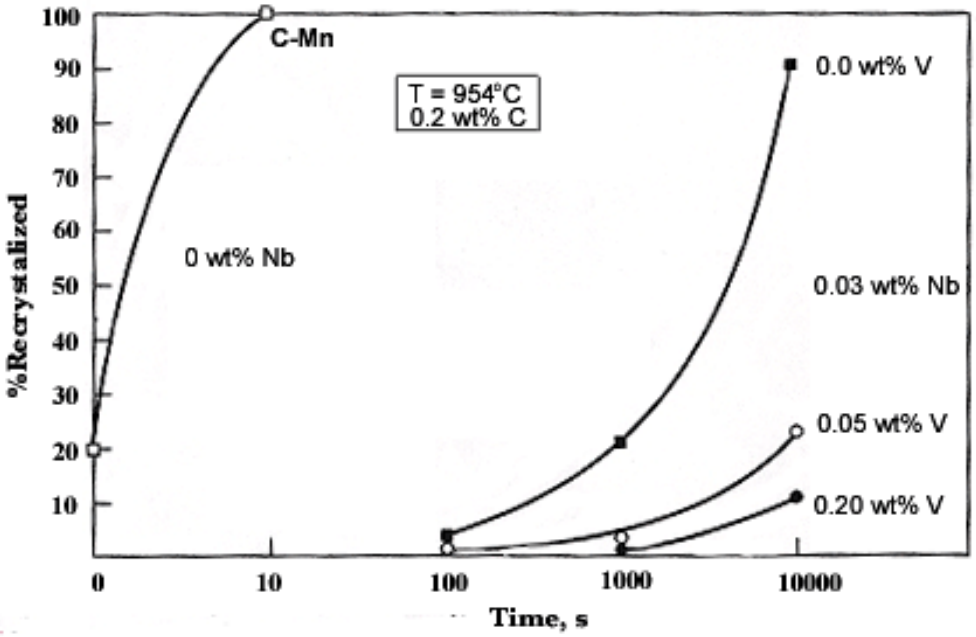

Figure 7. Recrystallization kinetics curves of four 0.1 wt.% C 0.2 wt.% Mn steels at 954 ^{o}C. The steel marked C-Mn had no microalloying addition. The others had 0.03 wt.% Nb plus the amounts of V indicated. Microalloying is seen to give a marked reduction in the recrystallization rate. (After Michael, et al. 31)

Ferrite: Grain growth is of crucial importance in the ferritic grain oriented iron-silicon electrical steels used in large power transformers. These electrical steels are unusual alloys based on Fe-3wt.% Si with at most hundredths of wt.% of either deliberate or trace alloying elements, except for Mn. The price of the steel is dictated by the core loss as determined by a simple measure, the Epstein test. These steels strictly fall outside the realm of this volume by never having existed in the austenitic state. However, studies on electrical steels provide invaluable guidance for grain growth in any ferritic steel.

The aim of the processing is then to produce thin (~0.3 mm) sheets of the steel with the minimum core loss. The details of the processing are closely guarded trade secrets, but the basics of the processing have become known from patents and the occasional paper by scientists at the steel companies. Leslie (32) stated in 1980 that "The processing of grain-oriented Si steels is the most complicated for any product in the industry." The physical phenomena responsible for the need of such sophistication are remarkable, and are still being discovered. Ushigami, et al. (33) and Suzuki, et al. (34) give review of recent developments in these steels.

The best electrical steels have a strong texture, named after the early investigator, Goss (35). In this {110}<100> texture the <100> direction is in the rolling direction and the {110} planes lie in the plane of the sheet. The grains are large, and extend all the way through the sheet.

Production of high quality sheet demands rigorous control of process variables (36). Typically, a 1350 ^{o}C soak is followed by a hot roll to ~2 mm, then a cold roll to final thickness. There may be an intermediate anneal during the cold rolling. The steel is then decarburized in wet H_2 at 800-850 ^{o}C, temperatures which give recrystallization but only limited grain growth. The steel is then given an insulating coating to prevent sticking during the final high temperature heat treatment and to give electrical insulation during use. The final processing step is a high temperature anneal at 1150 ^{o}C-1200 ^{o}C in dry H_2 where the final strong Goss texture is

obtained. The steel is ferritic at all stages in the processing. In fact the carbon content has to be kept low even before decarburization to prevent the formation of austenite during the processing cycle.

According to Humphreys and Hatherly (36) a few Goss grains are created during hot rolling. Subsequent processing induces these grains to predominate over all other possible textures and to grow to the proper grain size. This task is crucially dependent on the presence of fine (tens of nm diameter) MnS and/or AlN particles which serve to selectively pin the grain boundaries until they are coarsened/removed during the final anneal.

Lee and Szupnar (37) studied texture formation in a conventional grain oriented silicon steel, which used MnS for pinning. The alloy was decarburized in wet H_2 and then given secondary recrystallization anneals in helium. Figure 8 shows the development of the Goss texture at various annealing temperatures. The Goss texture does not much develop at 860 ^{o}C and below. Above this temperature the Goss grains proceed to dominate the microstructure. The Goss grains grow to much larger sizes than those of other orientations.

Lee and Szupnar (37) found a high frequency of Σ5 Coincidence Site Lattice (CSL) boundaries between the Goss grains and their neighbors, both before and after secondary recrystallization. They observed that the Σ5 CSL boundaries were highly mobile and concluded that the formation of Goss texture was strongly influenced by the presence of these boundaries.

Figure 9 shows schematically the sort of selective hindrance, which might lead to strong texture formation. The effectiveness of the hindrance would depend on the particle distribution on a given boundary as well as the effect of particle pinning on that particular grain boundary. There is an intermediate crucial hindrance range where selective pinning is effective. Secondary recrystallization of electrical steel must occur within that range to obtain the desired strong Goss texture.

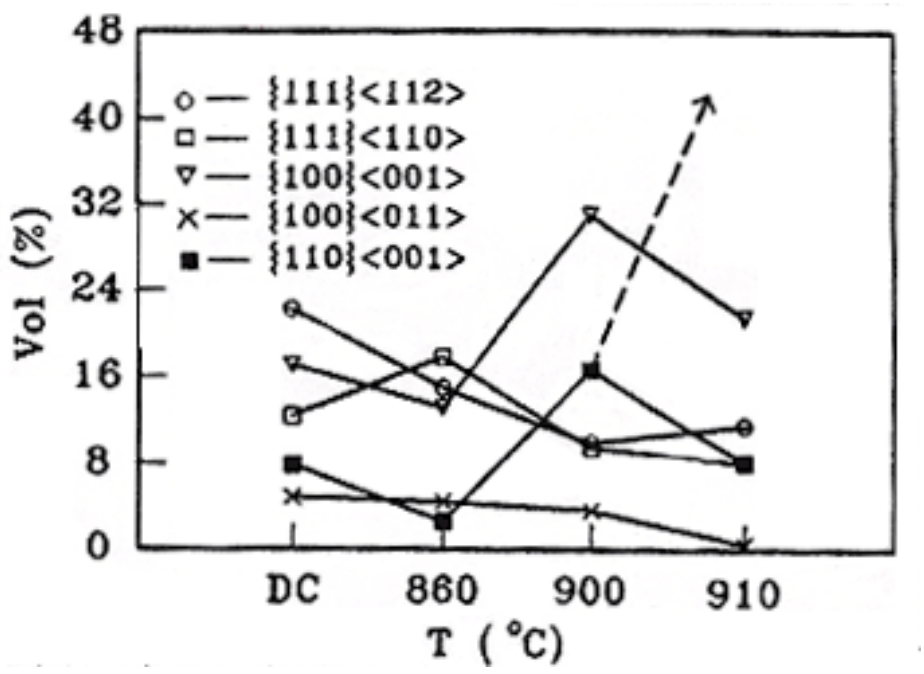

Figure 8. The effect of annealing temperature on the degree of dominance of Goss grains. Goss grains are seen to dominate the microstructure upon annealing at 900 ^{o}C and above. (After Lee and Szupnar 37)

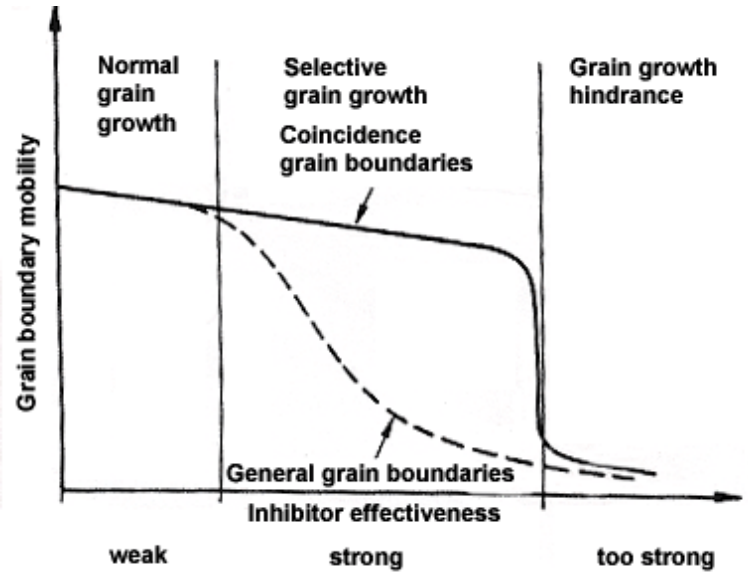

Figure 9. Relationship between grain boundary mobility and inhibitor effectiveness. For a limited range of conditions special boundaries are able to move rapidly while general grain boundaries are relatively immobile. (After Bölling, et al.38)

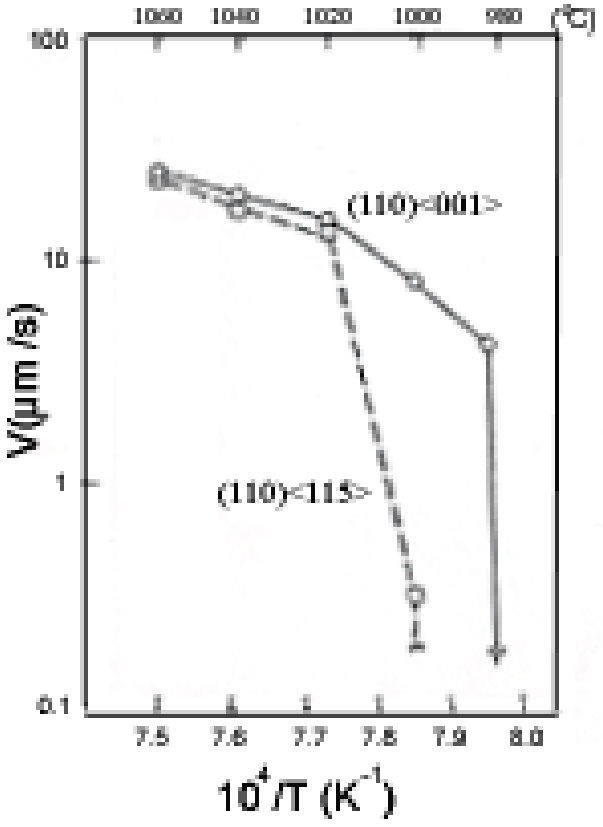

Figure 10. Comparison of growth rates of (110)<001> Goss Grains to (110)<115> grains. The Goss grains are seen to grow much faster above about 1020 ^{o}C. (After Ushigami, et al. 33)

Ushigami, et al. (33) show in Figure 10 that the Goss grains grow faster than (110)<115> grains. Accordingly, Goss grains could grow freely at temperatures where other grains were relatively immobile.

It is known that CSL boundaries are more highly ordered than "general" grain boundaries, which gives them unusual properties. Figure 11 from the classic study of Aust and Rutter (39, 40) shows this phenomenon. Special boundaries are seen to migrate much faster at a given temperature, and have a much lower activation energy for migration.

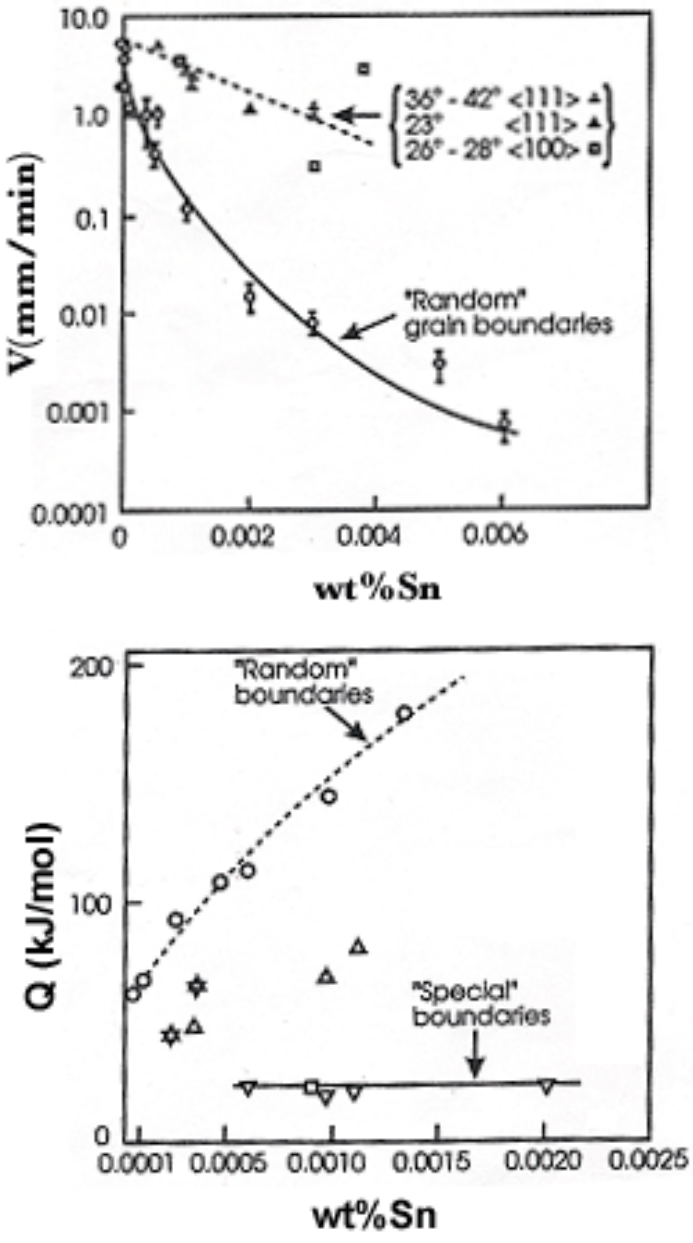

Figure 11. Grain boundary migrating at 300 ^{o}C in zone-refined lead crystals Special boundaries are found to: migrate much more rapidly at a given temperature (above) and have a lower activation energy for migration. (below) After Aust and Rutter 39, 40)

Ushigama, et al. (33) note that the lower grain boundary energies of special boundaries makes them less susceptible to Zener-Smith pinning. This lower energy also makes special boundaries less attractive sites for heterogeneous nucleation of second phase particles. As such, any special boundaries present when particle nucleation takes place would be less decorated than general boundaries. This lower pinning particle density would also contribute to the higher mobility of special boundaries. The so-called special boundaries thus have multiple roles in the control of the final recrystallized grain size and texture.

Summary

Compound precipitates have important roles in the processing and properties of steels. Both experimental and theoretical study of the coarsening kinetics of these particles are difficult tasks. Where critical tests were performed, good agreement was found between theory and experiment.

The effects of particle pinning and solute drag on grain boundary motion are hard to model or study. The role of special grain boundaries in grain growth is yet to be properly analyzed. The most promising development in the understanding of grain growth is provided by computer simulation. Better algorithms and greater computational capacity have made simulation of growth in 3-D possible, but only for pure, elemental crystals.

Particle pinning of grain boundaries is vital in controlling the grain size during high temperature processing of austenite. The particles may be aluminum nitrides formed in Al-killed plain carbon steels or refractory carbonitrides in HSLA steels. In any case the austenite grain size is much lower than in the absence of the particles.

Formation of the Goss texture in ferritic electrical steels depends on the selective growth of the desired grains. This is affected through the influence of MnS and/or AlN particles which retard migration of the Goss grains relatively little. Coarsening and dissolution of these particles during the final, high temperature anneal releases the more mobile Goss grains while the others are still pinned.

References

1. Fick, A. "Über Diffusion," *Poggendorff's Annalen*, 944 (1855) 59.
2. Zener, C.J. Theory of Growth of Spherical Precipitates From Solid Solution," J. Appl. Phys. 20 (1949) 950.
3. Greenwood, G.W. *Acta Metall*., "The Growth of Dispersed Precipitates in Solution." 4 (1956) 243-248.
4. Wagner, C. "Theorie der Alterung von Niederschlägen durch Umlösen" *Z. Elektrochem*. 65 (1961) 581-591.
5. Lifshitz, I.M. and V.V. Slyozov, "The Kinetics of Precipitation From Supersaturated Solid Solutions," *J. Phys. Chem. Solids* 91 (1961) 35-50.
6. Coble, R.L. Private Communication (1980)
7. Martin, J. W., R. D. Doherty, and B. Cantor, "Stability of Microstructures in Metallic Systems" Cambridge University Press, 1996.
8. Björklund, S.L.F. Donaghey and M. Hillert, The Effect of Alloying Elements on the Rate of Ostwald Ripening of Cementite in Steel," *Acta Metall*. 20 (1972) 867-874.
9. Bhattacharyya, S.K. and K.C. Russell "Activation Energies for the Coarsening of Compound Precipitates," *Met. Trans*. 3A (1972) 2195-2199.
10. Cochart, A. W. "Some Estimates of the Thermal Stability of Dispersion Hardened Alloys" Trans. *Metall. Soc. A.I.M.E*. 209 (1957) 434-437.

11. Lee, H.M., S.M. Allen, and M. Grujicic, Coarsening Resistance of M_2C Carbides in Secondary Hardening Steels: Part I. Theoretical Model for Multicomponent Coarsening Kinetics," *Metall. Trans*. 22A (1991) 2863-2868.
12. Burke, J.E. and D Turnbull *Progress in Metal Physics vol. 3* (London, Pergamon Press, Ltd. 1952) 220-292
13. Thompson, C.V. "Grain Growth and Evolution of Other Cellular Structures," *Solid State Physics vol. 55* (Academic Press, San Diego 2000) 270-314.
14. Hillert, M. "On the Theory of Normal and Abnormal Grain Growth," *Acta Metall*. 13 (1965) 227-238.
15. Smith, C.S. Trans. Metall. Soc. A.I.M.E. 175 (1948) 15.
16. Abbruzzese, G. and K. Lücke, "Theory of Grain Growth in the Presence of Second Phase Particles," *Materials Science Forum*, 94-96 (1992) 597-604.
17. Krill, C.E. III and L.-Q. Chen "Computer Simulation of 3-D Grain Growth Using a Phase-Field Model, " *Acta Materialia* 50 (2002) 3057-3073.
18. Cahn, J.W. "The Impurity-Drag Effect in Grain Boundary Motion, "*Acta Metall*. 10 (1962) 789-798.
19. Lücke, K. and H.P.Stüwe in *"Recovery and Recrystallization in Metals*,", L. Himmel, ed. (Interscience Publications, 1963) 171.
20. Bhattacharyya, S.K. and K.C. Russell "Coarsening Kinetics of Silica in Copper," *Met. Trans*. 7A (1976) 453-461.
21. Ozaki, Y. and T.H. Zee, "Coarsening of Hafnium Carbide Particles in Tungsten," *J. Mater. Sci*. 30 (1995) 3421-3428.
22. Hillert, M. "Pressure Induced Diffusion and Deformation During Precipitation, Especially Graphitization" Jernkont. Ann. 141 (1957) 157-181.
23. Gustafson, Å. "Coarsening of TiC in Austenitic Stainless Steel-Experiments and Simulations in Comparison," *Mater. Sci. Eng*. A287 (2000) 52-58.
24. Morral, J.E. and G.R. Purdy, "Particle Coarsening in Binary and Multicomponent Alloys," *Scripta Metall. et Met*. 30 (1994) 905-908.
25. Bain*, E.C., "Functions of the Alloying Elements in Steels*," (ASM, Cleveland, 1939).
26. Lee, H.M., S.M. Allen, and M. Grujicic, Coarsening Resistance of M_2C Carbides in Secondary Hardening Steels: Part II. Alloy Design Aided by a Thermochemical Database," *Metall. Trans*. 22A (1991) 2869-2876.
27. Lee, H.M., and S.M. Allen, "Coarsening Resistance of M_2C Carbides in Secondary Hardening Steels: Part III. "Comparison of Theory and Experiment," *Metall. Trans*. 22A (1991) 2877-2888.
28. Militzer, M., A. Giumelli, E.B. Hawbolt, and T.R. Meadowcroft, "Austenite Grain Growth Kinetics in Al-Killed Plain Carbon Steels," *Met. and Mater. Trans*. 27A (1996) 3399-3409.
29. Militzer, M. "Modeling of the Interaction of Precipitation and Grain Growth," in *Recrystallization and Grain Growth*, Eds. G. Gottstein and D.A. Molodov, (Springer-Verlag Berlin 2001) 361-366.
30. Hansen, S.S., J.B. Vander Sande, and M. Cohen "Niobium Carbonitride Precipitation and Austenite Recrystallization in Hot-Rolled Microalloyed Steels," *Metall. Trans*. 11A (1980) 387-402.
31. Michael, J.R., J.G. Speer, and S.S. Hansen, "Austenite Recrystallization in Niobium/Vanadium Microalloyed Steels,"*Met. Trans*. 18A (1987) 481.
32. Leslie, W.C. "*The Physical Metallurgy of Steels*," (Techbooks, Herndon, VA 1991, reprint of 1981 Hemisphere Pub. edition) 321.
33. Ushigami, K. Murakami, T. Kubota, "Analysis of Secondary Recrystallization in Grain Oriented Silicon Steel by Synchrotron X-Ray Topography" *Grain Growth in Polycrystalline Mateials III*, ed. H. Weiland, B.L. Adams, and A.D. Rollett, (Warrendale, PA Minerals, Metals, and Materials Society of AIME, 1998) 491-500

34. Suzuki, S. Y. Ushigami, H. Homma, S. Takebayashi, and T. Kubota, "Influence of Metallurgical Factors on Secondary Recrystallization of Silicon Steel," *Mater. Trans.* (Japan) 42 (2001) 994-1006.
35. Goss, N.P. *Trans. Am. Soc. Met*. 23 (1935) 511-576.
35. Humphreys, F.J. and M. Hatherly, "*Recrystallization and Related Annealing Phenomena*," (Elsevier, Oxford, 1996) 409.
37. Lee, K.T. and J.A. Szpunar, "The Role of Special Grain Boundaries During the Grain Growth in Fe-3%Si," *Canad. Metall. Quart*. 34 (1991) 257-262.
38. Bölling, F. K. Günther, A. Böttcher, and B. Hammer, "Trends in the Development of Grain-Oriented Electrical Sheet," *Mater. Tech., Steel Res*. 63 (1992) 408-412.
39. Aust, K.T. and J.W. Rutter "Grain Boundary Diffusion in High Purity Lead and Dilute Lead-Tin Alloys,"Trans. *Metall. Soc. A.I.M.E*. 215 (1959) 119-127
40. Aust, K.T. and J.W. Rutter "Temperature Dependence of Grain Migration in High Purity Lead Containing Small Additions of Tin," Trans. *Metall. Soc. A.I.M.E*. 215 (1959) 820-830.